Preparation of mitochondria to measure superoxide flashes and the mitochondrial permeability transition pore in angiosperm flowers

Chulan Zhang [Corresp.], **Fengshuo Sun** [1], **Biao Xiong** [2], **Zhixiang Zhang** [1]

[1] Beijing Forestry University (北京林业大学), Beijing, China

[2] Guizhou University, Guizhou, China

Corresponding Author: Chulan Zhang
Email address: janet311@sina.com

Background Mitochondria are the center of energy metabolism and the production of reactive oxygen species (ROS). ROS production results in a burst of “superoxide flashes”, which is always accompanied by opening of the mitochondrial permeability transition pore (mPTP). Superoxide flashes have only been studied in the model plant *Arabidopsis thaliana* using a complex method to isolate mitochondria. In this study, we present an efficient, easier method to isolate functional mitochondria from floral tissues to measure superoxide flashes and the mPTP.

Method We used 0.5 g samples to isolate mitochondria within < 1.5 h from flowers of two non-transgenic plants (*Magnolia denudata* and *Nelumbo nucifera*) to measure superoxide flashes and the mPTP. Superoxide flashes were visualized by the pH-insensitive indicator MitoSOX Red, while the mitochondrial membrane potential (ΔΨm) was labelled with TMRM.

Results Mitochondria isolated using our method showed a high respiration ratio. Our results indicate that the location of ROS and mitochondria was in a good coincidence. Increased ROS together with a higher frequency of superoxide flashes was found in the flower pistil. Furthermore, a higher rate of depolarization of the ΔΨm was observed in the pistil. Taken together, these results demonstrate that the frequency of superoxide flashes is closely related to depolarization of the ΔΨm in petals and pistils of flowers, and that the higher rate of mPTP activities was attributed to ion exchange in mitochondria.

Preparation of mitochondria to measure superoxide flashes and the mitochondrial permeability transition pore in angiosperm flowers

Chulan Zhang[1], Fengshuo Sun[2], Biao Xiong[3], and Zhixiang Zhang[1]

[1] College of Nature Conservation, Beijing Forestry University, Beijing, China

[2] College of Biological Sciences and Biotechnology, Beijing Forestry University, Beijing, China

[3] College of Tea Science, GuiZhou University, GuiZhou Province, China

Corresponding author:

Zhixiang Zhang, Ph.D.

Qinghua East Street, Beijing, 100083, China

E-mail: zxzhang@bjfu.edu.cn

Abstract

Background Mitochondria are the center of energy metabolism and the production of reactive oxygen species (ROS). ROS production results in a burst of "superoxide flashes", which is always accompanied by opening of the mitochondrial permeability transition pore (mPTP). Superoxide flashes have only been studied in the model plant *Arabidopsis thaliana* using a complex method to isolate mitochondria. In this study, we present an efficient, easier method to isolate functional mitochondria from floral tissues to measure superoxide flashes and the mPTP.
Method We used 0.5 g samples to isolate mitochondria within < 1.5 h from flowers of two non-transgenic plants (*Magnolia denudata* and *Nelumbo nucifera*) to measure superoxide flashes and the mPTP. Superoxide flashes were visualized by the pH-insensitive indicator MitoSOX Red, while the mitochondrial membrane potential ($\Delta\Psi m$) was labelled with TMRM.
Results Mitochondria isolated using our method showed a high respiration ratio. Our results indicate that the location of ROS and mitochondria was in a good coincidence. Increased ROS together with a higher frequency of superoxide flashes was found in the flower pistil. Furthermore, a higher rate of depolarization of the $\Delta\Psi m$ was observed in the pistil. Taken together, these results demonstrate that the frequency of superoxide flashes is closely related to depolarization of the $\Delta\Psi m$ in petals and pistils of flowers, and that the higher rate of mPTP activities was attributed to ion exchange in mitochondria.

Key words: isolation of mitochondria; mPTP; ROS; superoxide flashes

48

49

Introduction

51 Mitochondria are widely distributed organelles in eukaryotic cells where they perform
52 important roles generating energy, regulating physiological activities, and maintaining cellular
53 metabolism (Hatefi 1985; Yang et al. 2018). The major role of mitochondria is the generation of
54 ATP by oxidative phosphorylation through the electron transport chain (Hatefi 1985). In addition
55 to energy production, mitochondria are also the center of reactive oxygen species (ROS)
56 production in organisms under biotic or abiotic stress (Paital and Chainy 2014; Yang et al. 2016).
57 The isolation of mitochondria has deepened research on metabolism and stress in plants (Day et
58 al. 1985). In 1985, mitochondria from 300 g of pea leaves were isolated and purified by
59 centrifugation on a Percoll gradient containing a linear gradient of polyvinylpyrrolidone-25 (0–
60 10%, w/v) to obtain only 20 mg mitochondrial protein (Day et al. 1985). After that, mitochondria
61 were isolated from *Arabidopsis thaliana* using differential centrifugation and further purified
62 using a continuous colloidal density gradient (Lyu et al. 2018; Sweetlove et al. 2007). In
63 addition, crude isolation of mitochondria in leaves using density gradient centrifugation revealed
64 higher respiratory coupling than that observed in purified mitochondria (Keech et al. 2005). It is
65 well known that mitochondria must be purified to extract mitochondrial DNA and the proteome
66 (Ahmed and Fu 2015; Kim et al. 2015), but the time required and the sampling method were not
67 suitable in many mitochondrial studies, particularly in non-green tissues such as flowers. Crude
68 isolation of the intact and functional mitochondria is crucial for various studies in plants.

69

70 Superoxide flashes are 10-s events that occur spontaneously and suddenly in mitochondria
71 and reflect electrical and chemical activities (Feng et al. 2017). Superoxide flashes were first
72 defined as transient events of the mitochondrial matrix-targeted biosensor mt-cp YFP (Wei and
73 Dirksen 2012). As mt-cp YFP is sensitive to pH, superoxide flashes can be visualized by
74 chemical probes, including ROS indicators, such as MitoSOX for superoxide and 2.7-

dichlorodihyfrofluorescein (DCF) for H_2O_2 (Feng et al. 2017; Zhang et al. 2013). Interestingly, cp-YFP superoxide flashes are correlated with depolarization of the mitochondrial membrane potential ($\Delta\Psi_m$) (Zhang et al. 2013). The random opening and the small molecular leakage of the mitochondrial permeability transition pore (mPTP) were thought to ignite superoxide flashes (Hou et al. 2014). Previous studies have shown that ROS modulate a variety of physiological events, including growth, stress, thermogenesis, and diseases and trigger induction of the mitochondrial mPTP (Jastroch 2017; Keunen et al. 2015; Kuznetsov et al. 2017; Maksimov et al. 2018; Yang et al. 2016). It is clear that the accumulation of ROS and mPTP activity are closely associated with superoxide flashes. In animals, superoxide flashes and ROS bursts are involved in various physiological activities, such as oxidative stress, metabolism, and aging (Pouvreau 2010; Wei et al. 2011). Thus, there is a close relationship between superoxide flashes and mitochondrial energy metabolism. Considering the importance of the mitochondrial respiratory chain and energy metabolism, it is of great significance to study mitochondrial superoxide flashes in plants.

Superoxide flashes have been well studied in cells and isolated mitochondria of animals, and the cp YFP-flash signals are always associated with the loss of $\Delta\Psi_m$ (labeled with TMRM) (Li et al. 2012). Superoxide flashes loaded with the chemical probes MitoSOX and DCF reveal the same results and frequency as cp YFP flashes (Zhang et al. 2013). In plant tissues, superoxide flashes have only been studied in the roots of Arabidopsis and the cp-YFP signals changed with different respiratory substrates (Schwarzlander et al. 2011), but no study has explored superoxide flashes in other non-transgenic tissues of plants. Floral tissues in plants are important organs involved in various physical activities, including thermogenesis, pollination, and reproduction (Luo et al. 2010; Thien et al. 2009). Mitochondrial energy metabolism and oxygen consumption are closely related to floral thermogenesis and reproduction (Miller et al. 2011); thus, it is necessary to combine the activity of mitochondrial superoxide flashes with a study of floral reproduction in plants. As isolating plant mitochondria using a previous method was likely to

influence mitochondrial viability and the mitochondrial-targeted cp-YFP is hardly expressed in xylophyta flowers, a suitable method to study superoxide flashes and mPTP activity in floral tissues is crucial.

To address these issues, some important modifications were devised based on previous methods to study superoxide flashes (Zhang et al. 2013). We developed an efficient method to isolate mitochondria in flowers of *Magnolia denudata* and *Nelumbo nucifera*. As these are non-transgenic flowers, superoxide flashes were first visualized by loading the plants with MitoSOX Red, while the $\Delta\Psi_m$ was labelled with TMRM. These methods facilitated study of mitochondrial energy metabolism and physiological activities in non-transgenic flora of angiosperms. This quick and sample-saving protocol greatly improved the viability of mitochondria and efficiency of the experiment in non-green plant tissues.

Materials & Methods

Plant materials/plant growth

M. denudata was grown on the campus of Beijing Forestry University (40°00′02″N, 116°20′15″, a.s.l., 60 m). Pistils and petals of 15 flowers were collected during afternoons in March and April. *N. nucifera* was grown in Bajia Country Park (40°00′50″N, 116°19′39″E, a.s.l., 47 m). Receptacles and petals of nearly 10 flowers were collected during afternoons in July–August.

Solutions

Grinding buffer: 0.3 M sucrose, 25 mM $Na_4P_2O_4$, 2 mM EDTA, 10 mM KH_2PO_4, 1% (w/v) polyvinylpyrrolidone-40, 1% (w/v) defatted bovine serum albumin (BSA), 4 mM cysteine, and 20 mM ascorbic acid were added just prior to grinding. pH was adjusted to 7.5 with KOH. Resuspension buffer: 0.3 M sucrose, 10 mM N-Tris [hydroxymethyl]-methyl-2-aminoethanesulfonic acid (TES-KOH), and 0.1% BSA, pH = 7.5. Mitochondrial basic incubation

medium: 0.3 M sucrose, 10 mM TES-KOH. 10 mM NaCl, 5 mM KH_2PO_4, 2 mM $MgSO_4$, and 0.1% BSA, pH = 7.2

Isolation of mitochondria

All steps were carried at 4°C on ice. About 0.5 g of pistil or petal tissues were cut up from each species into 1 m^3 fragments with scissors. They were ground in 1–2 ml of grinding buffer using a pestle with a small amount of quartz. The extract was filtered through 20 μm nylon mesh and then centrifuged at 2,000 × g for 10 min to remove most of the thylakoid membranes and intact chloroplasts. The supernatant was transferred to a new tube and centrifuged at 12,000 × g for 20 min. The pellet was resuspended in 1 ml resuspension buffer and centrifuged for 5 min at 1,500 × g to remove the residual intact chloroplasts. The supernatant pellet was centrifuged for 20 min at 12,000 × g to yield the crude mitochondria. The crude mitochondria were suspended in mitochondrial basic incubation medium and placed on ice for further studies.

Mitochondrial respiratory function assay

The oxygen consumption rates of mitochondria were determined with a Clark-type oxygen electrode (Strathkelvin 782 2-Channel Oxygen System version 1.0, Strathkelvin Instruments, Motherwell, UK) at 25°C. A 10 μl aliquot of mitochondrial suspension was blended in 1 ml of mitochondrial basic incubation medium. The oxygen sensor signal was recorded on a computer at intervals of 0.5 s with Strathkelvin Instruments software (782 System version 1.0). Oxygen consumption was measured with 250 μM ADP (state 3) and with 5 mM succinate (state 4). The respiratory control ratio (RCR) was calculated as the ratio of state 3 to state 4 respiration. The mitochondrial suspension with higher than a state 3 RCR was used in subsequent studies.

Confocal imaging of Mito-ROS and mPTP

To visualize the superoxide flashes and $\Delta\Psi_m$, isolated mitochondria were immobilized on round glass cover slides (pretreatment with 0.2 mg/ml poly-L-lysine for 1 h; Sigma, St. Louis, MO, USA) by centrifugation at 2,000 × g for 5 min at 4°C and mounted on an inverted

157 microscope (Zeiss LSM 710: Carl Zeiss, Oberkochen, Germany) for imaging. To measure the
158 subcellular locations of mitochondria and ROS, mitochondria were first incubated with 100 nM
159 MitoTracker Green (Invitrogen, Carlsbad, CA, USA) for 30 min at 25°C and washed in
160 mitochondrial basic incubation medium, then loaded with 2.5 μM MitoSOX Red for 5 min.
161 MitoTracker Green was excited with 488 nm and emissions were collected at 500–530 nm, while
162 MitoSOX Red was excited with 543 nm and collected at an emission wavelength of 560–620
163 nm. Isolated mitochondria were labelled with 2.5 μM MitoSOX Red and 5 mM succinate as a
164 respiration substrate to measure superoxide flashes. Isolated mitochondria were loaded with 50
165 nM TMRM and 5 mM succinate for 1 min at 25°C to measure the $\Delta\Psi_m$. The excitation
166 wavelength for TMRM was 543 and the emission wavelength was 550–620 nm. A total of 100
167 frames of 512 × 512 pixels were collected for a typical time-series recording. The frame rate was
168 50–60 frames/min. All experiments were performed at room temperature (24–26°C).
169
170 **Data analysis**
171 The images obtained by laser scanning confocal microscopy were analyzed using Image J
172 1.48v (Wayne Rasband, National Institutes of Health, Bethesda, MD, USA). Superoxide flashes
173 and variations in the $\Delta\Psi_m$ were identified using FlashSniper (Li et al. 2012), and their
174 morphological, properties, and duration were measured automatically. Statistical analyses were
175 performed using SPSS Statistics 23.0 software (IBM Corp., Armonk, NY, USA). Images were
176 processed and assembled using Adobe Photoshop CS 5 (Adobe Systems Corp., San Jose, CA,
177 USA).
178
179
180
181 ## Results
182 **Respiratory function and viability of isolated mitochondria**
183 Crude mitochondria were sampled from flower, petal, and style tissues of magnolia as

shown in Fig. 1a, while the petal and receptacle tissues of lotus were sampled as shown in Fig. 1f. A signal with excitation at 488 nm was confirmed to avoid disturbing the auto-fluorescence of intact chloroplasts. As shown in Fig. 1b and g, no intact chloroplasts were detected in the crude isolated mitochondria. To compare the previous method (method B) (Day et al. 1985) and our efficient method (method A) to isolate mitochondria, the respiratory function of the isolated mitochondria was determined with a Clark-type oxygen electrode. As a result, the RCR did not change significantly in mitochondria isolated from flowers using method A (n = 6), but RCR declined in isolated mitochondria using method B (n = 6) (Table 1). As the viability of mitochondria is reflected by the $\Delta\Psi_m$, crude isolated mitochondria were loaded with the TMRM indicator. Highly viable and highly dense mitochondria were observed in tissues of magnolia (Fig. 1c, d) and lotus (Fig. 1h, i). The viability of mitochondria using method B was lower than that of method A (Fig. 1e, j). We assessed the time consumed, amount of sample consumed, and the viability of both methods. Method B was processed in 5.28 ± 0.23 h and consumed 43.92 ± 3.78 g of flower tissues (n = 6), whereas mitochondria were isolated within 1.13 ± 0.14 h with only 0.47 ± 0.12 g tissues (n = 6) using our method A. This result shows that our mitochondrial isolation method was highly efficient to obtain highly viable mitochondria in the flower species.

ROS activity in floral mitochondria

To identify the intracellular site of ROS production, mitochondrial ROS were loaded with MitoSOX Red for 5 min (2.5 μM), while mitochondria were loaded with Mito Tracker Green for 30 min (100 nM). ROS production and mitochondrial location were coincident in the petals and styles of magnolia, suggesting that mitochondria are the primary site of ROS production in this species (Fig. 2A-c, f). The same results were found in the receptacle and petal of lotus (Fig. 2C-c, f).

The fluorescent level of mitochondrial ROS increased significantly in the style compared to the petal of magnolia (Fig A-b, e, and B) (n = 100). In addition, similar results were found in the mitochondria of lotus, as the ROS level was significantly higher in the receptacle than in the

petal (Fig C-b, e and D) (n = 100). Our results confirm that mitochondrial ROS tended to accumulate in the pistil of both magnolia and lotus, indicating that mitochondrial ROS might be more involved in the electron transport chain in the pistil than in the petal.

Superoxide flashes in flowers

To investigate the nature of superoxide flashes in magnolia and lotus, mitochondria were loaded with the ROS fluorescent probe MitoSOX Red with 5 mM succinate added as respiratory substrate. According to a previous study (Wang et al. 2016b), we defined the variation of fluorescence at $df/F_0 > 0.2$ within 10 s as a single superoxide flash event. A transient increase in MitoSOX fluorescence and variations in the trace were observed during 100 s in single mitochondrial events (Fig. 3A, B, and Online Resource 1). Among these instantaneous traces, three types of mitochondrial superoxide traces were classified (Fig. 3C): low variation slope traces ($0.2 < df/F_0 < 0.5$) (Fig. 3C-a), high variation slope traces ($0.5 \leq df/F_0$) (Fig. 3C-b), and multi-event traces ($0.2 < df/F_0$) (Fig. 3C-c). We also compared the frequency of superoxide flashes (/100s ×1,000 μm^2) in petals and pistils of magnolia and lotus. Notably, superoxide oxide flashes labelled with MitoSOX Red were detected at a rate of 129.18 ± 20.11 (/100 s ×1,000 μm^2, n = 13) in the magnolia style (Fig. 3D-a) which was significantly higher than the petal (75.23 ± 10.48/100 s ×1,000 μm^2, n = 11). In lotus (Fig. 3D-b), the rate of superoxide flashes was 48.24 ± 10.24 (/100 s × 1,000 μm^2, n = 10) in the receptacle, which was also significantly higher than the petal (25.68 ± 4.79 /100 s × 1,000 μm^2, n = 10). These results indicate that superoxide flashes, together with ROS bursts, are highly autonomous and predominantly reflect the properties and physical activities of mitochondria in different tissues and species.

Depolarization of the mitochondrial membrane potential in flowers

To study variations in the $\Delta\Psi_m$, isolated mitochondria were labelled with TMRM, and 5 mM of succinate was added. The decline in fluorescent intensity at $df/F_0 < -0.2$ was defined as an event. Transient depolarization of the $\Delta\Psi m$ accompanied by later polarization occurred in a

single mitochondrion (Fig. 4A, B and Online Resource 2). According to the wide variation in ΔΨm, the trace ΔΨm was catalogued into three types (Fig. 4C): Instantaneous loss of ΔΨm along with instant recovery (Fig. 4C-a), instantaneous loss of ΔΨm with a short period of stability before recovery (Fig. 4C-b), and multi-event trace including the above two types (Fig. 4C-c). The frequency of a TMRM-event in magnolia petals (544.92 ± 56.98 /100 s ×1,000 μm^2, n = 15) was significantly lower than the values in the style (1,009.10 ± 130.10 /100 s ×1,000 μm^2, n = 15) (Fig. 4D-a). The same result was found in lotus (Fig. 4D-b) that the frequency of TMRM events in the lotus petal was 51.94 ± 10.57 (/100 s × 1,000 μm^2, n = 10) which was lower than that in the receptacle (119.99 ± 19.00 /100 s ×1,000 μm^2, n = 10). We conclude that transient and spontaneous depolarization of ΔΨm occurred in all tissues and the higher frequency of variation of ΔΨm in the pistils of flowers suggest that they have a higher level of mitochondrial dynamics.

Discussion

Isolating mitochondria from plant tissues is complex and inefficient. In a previous study, the sucrose-based differential centrifugation method requires high-speed centrifugation (40,000 × g) and 300 g of sample within 5 h to obtain purified mitochondria (Day et al. 1985). Isolating mitochondria using the colloidal density gradient method consumes 60 g of sample and more than 4 h (Sweetlove et al. 2007). These methods are time- and sample-consuming, which may hinder the function and respiratory coupling of the mitochondria. In our method, we used only 0.5 g of floral tissues to obtain crude functional mitochondria in less than 1.5 h after centrifugation at a low speed (≤12,000 × g), which only required a standard laboratory centrifuge. A previous study reported that isolating crude mitochondria from leaves results in a higher RCR than when isolating purified mitochondria, which was consistent with our results (Keech et al. 2005). In the present study, we provide an effective and simple method to obtain highly viable mitochondria in different flower tissues to measure superoxide flashes and the $\Delta\Psi_m$.

ROS modulate various physiological events, including stress, growth, and cell death (Dickinson and Chang 2011; NavaneethaKrishnan et al. 2018; Sundaresan et al. 1995). ROS sustain the polar growth of cells, such as root hairs and pollen tubes, and have a strong impact on cell wall properties (Mangano et al. 2016). Colocalization of ROS and mitochondria in polar growing pollen tubes reveals the production of H_2O_2 in mitochondria during pollen germination (Maksimov et al. 2018). Colocalization of ROS and mitochondria was observed in salt-treated tobacco cells (de la Garma et al. 2015). Moreover, ROS are produced in mitochondria until the full flower bloom stage (Chakrabarty et al. 2007; Rogers 2012). Our study found good coincidence between the location of ROS and mitochondria in petals and pistils of two flower species (Fig. 2), indicating that ROS originate in mitochondria from floral tissues. Overproduction of ROS leads to cell and tissue dysfunction, so ROS act as signal to alter the entire physiology of the plant cell (Monaghan et al. 2009; Navrot et al. 2007). ROS act as signaling molecules to unlock the antioxidant system and maintain physiological activities in plants under salt stress (Ahanger et al. 2017). ROS are also involved in the energy-dissipating system that increases frost resistance in seedlings under freezing conditions (Grabelnych et al. 2014). Moreover, mitochondria contribute to ROS production through electron transfer from the respiratory chain in non-green tissues, such as flowers, and ROS homeostasis is regulated by the antioxidant system (Rhoads et al. 2006; Rogers and Munne-Bosch 2016). Considering the increased ROS production in pistils of magnolia and lotus in our study, mitochondrial ROS might be more involved in the respiratory metabolic signaling pathways in the pistils of these two flower species.

An increase in ROS accumulation can trigger ROS burst in plants (Zandalinas and Mittler 2018), and basal mitochondrial ROS production is intimately linked with ROS flashes (Wang et al. 2012). The basal elevation of mitochondrial ROS and mitochondrial Ca^{2+} triggers superoxide flashes (Hou et al. 2013a). In addition, global ROS participate in modulating ROS flashes that are inhibited by antioxidants (Ma et al. 2011; Zhang et al. 2013). In our results, the simultaneous increase in ROS production and the frequency of superoxide flashes in the pistils indicated that

increasing ROS production might trigger superoxide flashes. Superoxide flashes are involved in various stressful and pathophysiological conditions (Fang et al. 2011; Wang et al. 2013). Superoxide flashes are sensitive to mitochondrial respiration and a higher frequency of superoxide flash events acts as an early mitochondrial signal in response to physiological activities and oxidative stress (Ma et al. 2011; Wei et al. 2011). Superoxide flashes always respond to metabolic activities and act as a signal mediating disease (Cao et al. 2013; Wang et al. 2013). In addition, the frequency of superoxide flashes in early adulthood predicts the lifespan of an organism (Shen et al. 2014). Furthermore, a deficiency in the mitochondrial fusion protein OPA1 decreases the frequency of superoxide flashes due to changes in the respiratory chain, suggesting that superoxide flashes participate in regulating mitochondrial fusion (Li et al. 2016; Rosselin et al. 2017). Similarly, changes in superoxide flashes and fluorescence are closely related to respiratory activity in Arabidopsis and are affected by different respiratory substrates and inhibitors (Schwarzlander et al. 2011). Considering that superoxide flashes visualized by MitoSOX occurred at a similar frequency as cp-YFP-flashes in previous studies (Wang et al. 2016a; Zhang et al. 2013), our findings show that MitoSOX flashes in flower tissues reflect the nature of the flashes. An increase in the frequency of flashes in the pistil indicates that superoxide flashes together with mitochondrial ROS might be more involved in mitochondrial viability and physiological metabolism in flower pistils.

Spontaneous burst superoxide flashes are always consequential to transient opening of the mitochondrial mPTP (Feng et al. 2017). A cp-YFP flash is always accompanied by depolarization of the $\Delta\Psi m$ (Li et al. 2012). Superoxide flashes are ignited by opening of the mPTP, and inhibiting mPTP-mediated superoxide flashes prevents normal physiological activities (Hou et al. 2013b; Wang et al. 2012). The global rise in mitochondrial basal ROS can trigger induction of the mPTP (Zorov et al. 2014) with further stimulation of ROS-induced ROS release resulting in an amplified ROS signal in response to oxidative challenge (Kuznetsov et al. 2017). Reversible opening of the mPTP is associated with the release of ROS and Ca^{2+} sparks under different physiological conditions (Kuznetsov et al. 2017). The simultaneous change in the

frequency of superoxide flashes and depolarization of the mPTP in our study suggest that superoxide flashes are always accompanied by fluctuations in the ΔΨm. Although the biogenesis of superoxide flashes is closely related to depolarization of the mPTP, the genesis of the flashes is not only related to ΔΨm fluctuations. The incidence of ΔΨm fluctuations is higher than that of superoxide flashes, because the cation and anion channels potentially contribute to fluctuation in the ΔΨm (Wang et al. 2012). Moreover, opening of the mPTP dissipates the electrochemical proton gradient, relying on mitochondrial Ca^{2+} concentration and matrix alkalization (Andrienko et al. 2017; Ponnalagu and Singh 2017). Thus, the higher rate of depolarization of ΔΨm in our study suggests more ion exchange in mitochondria than the incidence of flashes.

Conclusions

In conclusion, our study presents an efficient method to isolate functional mitochondria to study superoxide flashes and the mPTP. Superoxide flashes visualized by MitoSOX reflect the nature of the flash. Moreover, the simultaneous increase in MitoSOX flashes and opening of the mPTP in pistils demonstrate that mitochondria are involved in energy metabolism and physiological activities. The higher rate of fluctuation in the ΔΨm was attributed to the exchange of ions in the mPTP other than the incidence of flashes.

Acknowledgements

This study was supported by the National Natural Science Foundation of China (No. J 1310002).

Figure legends

Table 1 Respiratory function of isolated mitochondria with our method A and previous method B.

Values are mean ± S.D., n=6.

Fig. 1 Sampling and detection of isolated mitochondria. Sampling of *Magnolia denudata* (a) and *Nelumbo nucifera* (f). Detection of auto-fluorescence of intact chloroplasts in *M. denudata* (b) and *N. nucifera* (g). Viability of isolated mitochondria in petal (c) and style (d) of *M. denudata*, petal (h) and receptacle (i) of *N. nucifera* using method A. Viability of isolated mitochondria in *M. denudata* (e) and *N. nucifera* (j) using method B. Pe: petal, Gy: gynoecium, Rec: receptacle. Scale bar: 5μm.

Fig. 2 ROS production and colocalization with mitochondria. A. ROS production and colocalization with mitochondria in *M. denudata*: mitochondria were visualized by Mito Tracker

Green (in green color) in petal (a) and style (d), mitochondrial ROS was visualized by MitoSOX red (in red color) in petal (b) and style (e), colocalization of ROS and mitochondria in petal (c) and style (f). B. Comparison of ROS fluorescent intensity in petal and style of *M. denudata*. C. ROS production and colocalization with mitochondria in *N. nucifera*: mitochondria were visualized by Mito Tracker Green (in green color) in petal (a) and receptacle (d), mitochondrial ROS was visualized by MitoSOX red (in red color) in petal (b) and receptacle (e), colocalization of ROS and mitochondria in petal (c) and receptacle (f). D. Comparison of ROS fluorescent intensity in petal and receptacle of *N. nucifera*. Scale bar: 5μm.

Fig. 3 Superoxide flashes visualized by MitoSOX and flashes frequency. A. Isolated mitochondria labeled with MitoSOX red. B. Time-lapse images (upper) and typical trace (lower panel) of superoxide flashes visualized by MitoSOX red. C. Different types of traces of superoxide flashes (a) low variation slope traces, (b) high variation slope traces, (c) multi-event traces. D. Comparison of superoxide flashes frequency in petal and style of *M. denudata* (a). Comparison of superoxide flashes frequency in petal and receptacle of *N. nucifera* (b). Scale bar: 5μm.

Fig. 4 Depolarization of mitochondria membrane potential (ΔΨm) and frequency. A. Isolated mitochondria labeled by TMRM. B. Time-lapse images (upper) and typical trace (lower panel) of depolarization of ΔΨm labeled by TMRM. C. Different types of trace of TMRM (a) instantaneous loss and recovery of ΔΨm, (b) instantaneous loss with the short period of stability before recovery of ΔΨm (c) multi-event traces. D. Comparison of depolarization of ΔΨm frequency in petal and style of *M. denudata*. (a). Comparison of depolarization of ΔΨm frequency in petal and receptacle of *N. nucifera* (b). Scale bar: 5μm.

References

Ahanger MA, Tomar NS, Tittal M, Argal S, Agarwal RM (2017) Plant growth under water/salt stress: ROS production; antioxidants and significance of added potassium under such conditions. Physiol Mol Biol Pla 23:731-744

Ahmed Z, Fu YB (2015) An improved method with a wider applicability to isolate plant mitochondria for mtDNA extraction. Plant methods 11:56

Andrienko TN, Pasdois P, Pereira GC, Ovens MJ, Halestrap AP (2017) The role of succinate and ROS in reperfusion injury - A critical appraisal. J Mol Cell Cardiol 110:1-14

Cao YX et al. (2013) Proinflammatory cytokines stimulate mitochondrial superoxide flashes in articular chondrocytes in vitro and in situ. PloS One 8:e66444

Chakrabarty D, Chatterjee J, Datta SK (2007) Oxidative stress and antioxidant activity as the basis of senescence in chrysanthemum florets. Plant Growth Regul 53:107-115

de la Garma JG, Fernandez-Garcia N, Bardisi E, Pallol B, Rubio-Asensio JS, Bru R, Olmos E (2015) New insights into plant salt acclimation: the roles of vesicle trafficking and reactive oxygen species signalling in mitochondria and the endomembrane system. New Phytol 205:216-239

Day DA, Neuburger M., Douce R (1985) Biochemical characterrization of chlorophyll-free mitochondria from pea leaves. Aust J Plant Physio 12:219-228

Dickinson BC, Chang CJ (2011) Chemistry and biology of reactive oxygen species in signaling or stress responses. Nat Chem Biol 7:504-511

Fang HQ et al. (2011) Imaging superoxide flash and metabolism-coupled mitochondrial permeability transition in living animals. Cell Res 21:1295-1304

Feng G, Liu B, Hou T, Wang X, Cheng H (2017) Mitochondrial flashes: elemental signaling events in eukaryotic cells. Handb Exp Pharmacol 240:403-422

Grabelnych OI et al. (2014) Mitochondrial energy-dissipating systems (alternative oxidase, uncoupling proteins, and external NADH dehydrogenase) are involved in development of frost-resistance of winter wheat seedlings. Biochemistry-Moscow+ 79:506-519

Hatefi Y (1985) The mitochondrial electron transport and oxidative phosphorylation system. Annu Rev of Biochem 54:1015-1069

Hou TT et al. (2013a) Synergistic triggering of superoxide flashes by Mmtochondrial Ca^{2+} uniport and basal reactive oxygen species elevation. J Biol Chem 288:4602-4612

Hou Y, Ghosh P, Wan R, Ouyang X, Cheng H, Mattson MP, Cheng A (2014) Permeability transition pore-mediated mitochondrial superoxide flashes mediate an early inhibitory effect of amyloid beta1-42 on neural progenitor cell proliferation. Neurobiol Aging 35:975-989

Hou Y, Mattson MP, Cheng AW (2013b) Permeability transition pore-mediated mitochondrial superoxide flashes regulate cortical neural progenitor differentiation. PloS One 8:e76721

Jastroch M (2017) Uncoupling protein 1 controls reactive oxygen species in brown adipose tissue. Proc Natl Acad Sci U S A 114:7744-7746

Keech O, Dizengremel P, Gardestrom P (2005) Preparation of leaf mitochondria from *Arabidopsis thaliana*. Physiol Plantarum 124:403-409

Keunen E, Schellingen K, Van Der Straeten D, Remans T, Colpaert J, Vangronsveld J, Cuypers A (2015)

Alternative oxidase1a modulates the oxidative challenge during moderate Cd exposure in *Arabidopsis thaliana* leaves. J Exp Bot 66:2967-2977

Kim HY, Botelho SC, Park KJ, Kim H (2015) Use of carbonate extraction in analyzing moderately hydrophobic transmembrane proteins in the mitochondrial inner membrane. Protein Sci 24:2063-2069

Kuznetsov AV, Javadov S, Saks V, Margreiter R, Grimm M (2017) Synchronism in mitochondrial ROS flashes, membrane depolarization and calcium sparks in human carcinoma cells. Biochimica et biophysica acta 1858:418-431

Li K et al. (2012) Superoxide flashes reveal novel properties of mitochondrial reactive oxygen species excitability in cardiomyocytes. Biophys J 102:1011-1021

Li WW et al. (2016) Regulation of mitoflash biogenesis and signaling by mitochondrial dynamics. Sci Rep-Uk 6

Luo SX, Chaw SM, Zhang DX, Renner SS (2010) Flower heating following anthesis and the evolution of gall midge pollination in Schisandraceae. Am J Bot 97:1220-1228

Lyu W, Selinski J, Li L, Day DA, Murcha MW, Whelan J, Wang Y (2018) Isolation and respiratory measurements of mitochondria from *Arabidopsis thaliana*. J Vis Exp 131:e56627

Ma Q et al. (2011) Superoxide flashes early mitochondrial signals for oxidative stress-induced apoptosis. J Biol Chem 286:27573-27581

Maksimov N, Evmenyeva A, Breygina M, Yermakov I (2018) The role of reactive oxygen species in pollen germination in *Picea pungens* (blue spruce). Plant reproduction

Mangano S, Juarez SPD, Estevez JM (2016) ROS regulation of polar growth in plant cells. Plant Physiol 171:1593-1605

Miller RE, Grant NM, Giles L, Ribas-Carbo M, Berry JA, Watling JR, Robinson SA (2011) In the heat of the night - alternative pathway respiration drives thermogenesis in *Philodendron bipinnatifidum*. New Phytol 189:1013-1026

Monaghan P, Metcalfe NB, Torres R (2009) Oxidative stress as a mediator of life history trade-offs: mechanisms, measurements and interpretation. Ecol Lett 12:75-92

NavaneethaKrishnan S, Rosales JL, Lee KY (2018) Loss of Cdk5 in breast cancer cells promotes ROS-mediated cell death through dysregulation of the mitochondrial permeability transition pore. Oncogene 37:1788-1804

Navrot N, Rouhier N, Gelhaye E, Jacquot JP (2007) Reactive oxygen species generation and antioxidant systems in plant mitochondria. Physiol Plantarum 129:185-195

Paital B, Chainy GB (2014) Effects of temperature on complexes I and II mediated respiration, ROS generation and oxidative stress status in isolated gill mitochondria of the mud crab *Scylla serrata*. J Therm Biol 41:104-111

Ponnalagu D, Singh H (2017) Anion channels of mitochondria. Handb Exp Pharmacol 240:71-101

Pouvreau S (2010) Superoxide flashes in mouse skeletal muscle are produced by discrete arrays of active mitochondria operating coherently. PloS One 5:4439-4451

Rhoads DM, Umbach AL, Subbaiah CC, Siedow JN (2006) Mitochondrial reactive oxygen species. Contribution to oxidative stress and interorganellar signaling. Plant Physiol 141:357-366

Rogers H, Munne-Bosch S (2016) Production and scavenging of reactive oxygen species and redox signaling during leaf and flower senescence: similar but different. Plant Physiol 171:1560-1568

Rogers HJ (2012) Is there an important role for reactive oxygen species and redox regulation during floral senescence? Plant Cell Environ 35:217-233

Rosselin M, Santo-Domingo J, Bermont F, Giacomello M, Demaurex N (2017) L-OPA1 regulates mitoflash biogenesis independently from membrane fusion. Embo Rep 18:451-463

Schwarzlander M, Logan DC, Fricker MD, Sweetlove LJ (2011) The circularly permuted yellow fluorescent protein cpYFP that has been used as a superoxide probe is highly responsive to pH but not superoxide in mitochondria: implications for the existence of superoxide 'flashes'. Biochem J 437:381-387

Shen EZ et al. (2014) Mitoflash frequency in early adulthood predicts lifespan in *Caenorhabditis elegans*. Nature 508:128-132

Sundaresan M, Yu ZX, Ferrans VJ, Irani K, Finkel T (1995) Requirement for generation of H_2O_2 for platelet-derived growth factor signal transduction. Science 270:296-299

Sweetlove LJ, Taylor NL, Leaver CJ (2007) Isolation of intact, functional mitochondria from the model plant *Arabidopsis thaliana*. Methods Mol Biol 372:125-136

Thien LB et al. (2009) Pollination biology of basal angiosperms (Anita Grade). Am J Bot 96:166-182

Wang JQ et al. (2013) Dysregulation of mitochondrial calcium signaling and superoxide flashes cause mitochondrial genomic DNA damage in Huntington Disease. J Biol Chem 288:3070-3084

Wang W, Gong GH, Wang XH, Wei-LaPierre L, Cheng HP, Dirksen R, Sheu SS (2016a) Mitochondrial flash: integrative reactive oxygen species and pH signals in cell and organelle biology. Antioxid Redox Sign 25:534-549

Wang X et al. (2012) Superoxide flashes: elemental events of mitochondrial ROS signaling in the heart. J Mol Cell Cardiol 52:940-948

Wang XH et al. (2016b) Protons trigger mitochondrial flashes. Biophys J 111:386-394

Wei L, Dirksen RT (2012) Perspectives on: SGP symposium on mitochondrial physiology and medicine: mitochondrial superoxide flashes: from discovery to new controversies. J Gen Physiol 139:425-434

Wei L, Salahura G, Boncompagni S, Kasischke KA, Protasi F, Sheu SS, Dirksen RT (2011) Mitochondrial superoxide flashes: metabolic biomarkers of skeletal muscle activity and disease. Faseb J 25:3068-3078

Yang JL, Mukda S, Chen SD (2018) Diverse roles of mitochondria in ischemic stroke. Redox biology 16:263-275

Yang Y, Karakhanova S, Hartwig W, D'Haese JG, Philippov PP, Werner J, Bazhin AV (2016) Mitochondria and mitochondrial ROS in cancer: novel targets for anticancer therapy. J Cell Physiol 231:2570-2581

Zandalinas SI, Mittler R (2018) ROS-induced ROS release in plant and animal cells. Free Radical Bio Med 122:21-27

Zhang X et al. (2013) Superoxide constitutes a major signal of mitochondrial superoxide flash. Life sciences 93:178-186

Zorov DB, Juhaszova M, Sollott SJ (2014) Mitochondrial reactive oxygen species (Ros) and Ros-Induced Ros Release. Physiol Rev 94:909-950

Figure 1

Sampling and detection of isolated mitochondria.

Sampling of *Magnolia denudata* (a) and *Nelumbo nucifera* (f). Detection of auto-fluorescence of intact chloroplasts in *M. denudata* (b) and *N. nucifera* (g). Viability of isolated mitochondria in petal (c) and style (d) of *M. denudata*, petal (h) and receptacle (i) of *N. nucifera* using method A. Viability of isolated mitochondria in *M. denudata* (e) and *N. nucifera* (j) using method B. Pe: petal, Gy: gynoecium, Rec: receptacle. Scale bar: 5μm.

**Note: Auto Gamma Correction was used for the image. This only affects the reviewing manuscript. See original source image if needed for review.*

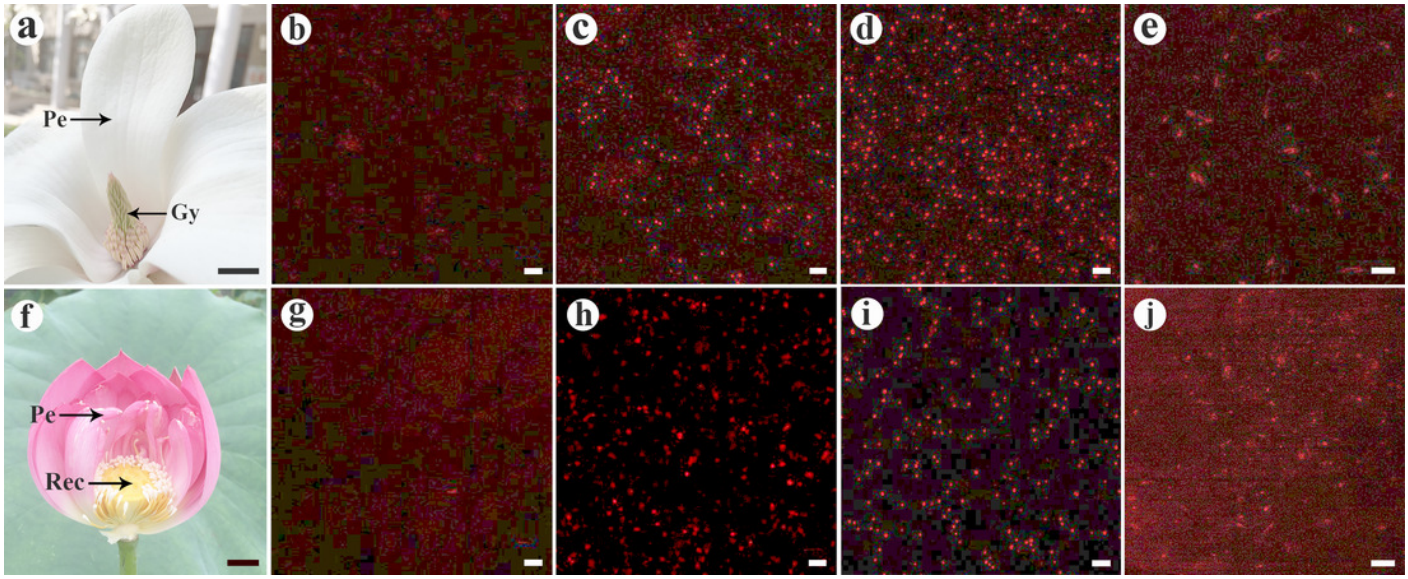

Figure 2

ROS production and colocalization with mitochondria

A. ROS production and colocalization with mitochondria in *M. denudata*: mitochondria were visualized by Mito Tracker Green (in green color) in petal (a) and style (d), mitochondrial ROS was visualized by MitoSOX red (in red color) in petal (b) and style (e), colocalization of ROS and mitochondria in petal (c) and style (f). B. Comparison of ROS fluorescent intensity in petal and style of *M. denudata*. C. ROS production and colocalization with mitochondria in *N. nucifera*: mitochondria were visualized by Mito Tracker Green (in green color) in petal (a) and receptacle (d), mitochondrial ROS was visualized by MitoSOX red (in red color) in petal (b) and receptacle (e), colocalization of ROS and mitochondria in petal (c) and receptacle (f). D. Comparison of ROS fluorescent intensity in petal and receptacle of *N. nucifera*. Scale bar: 5μm.

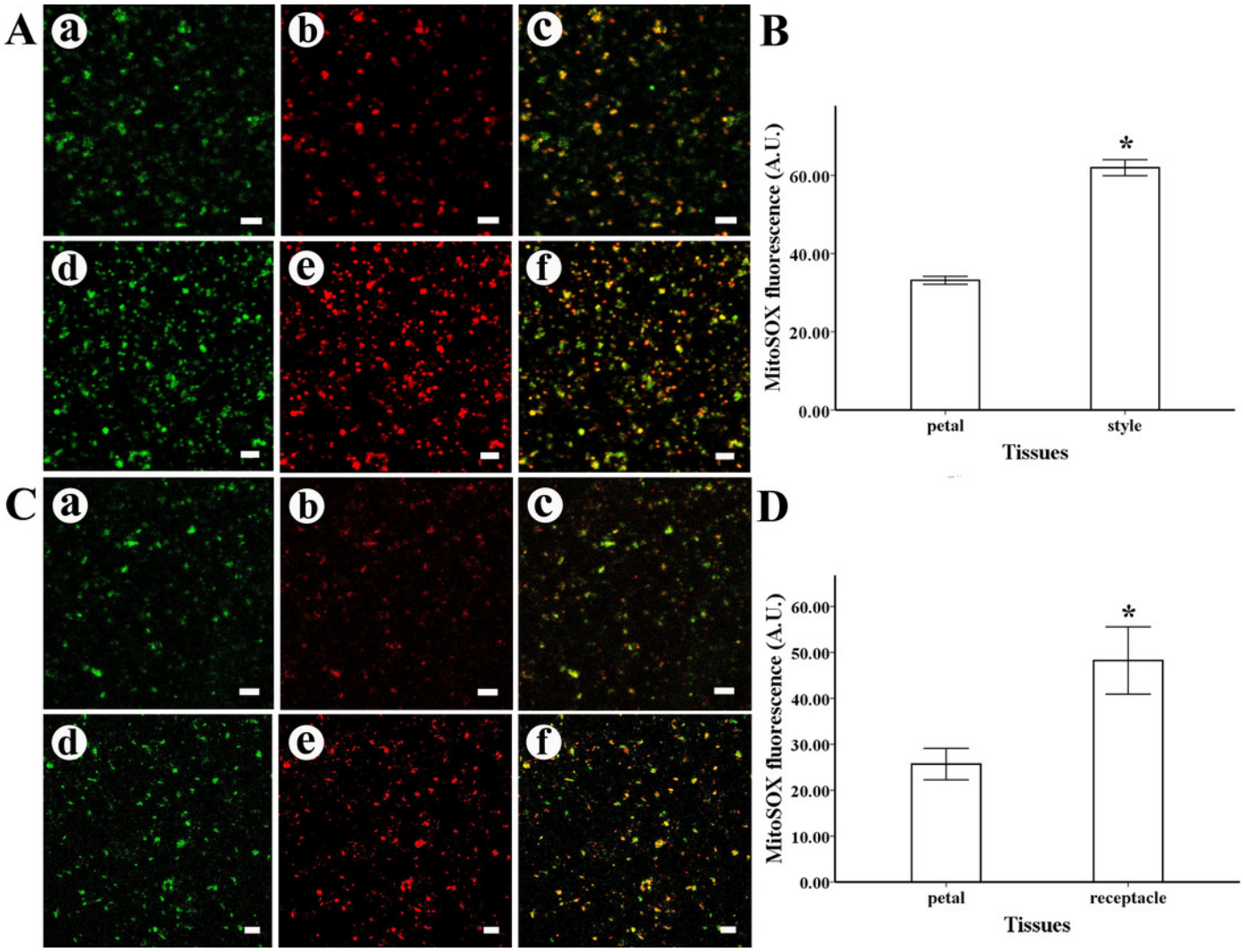
A
a
b
c
d
e
f
B
MitoSOX fluorescence (A.U.)
0.00
20.00
40.00
60.00
*
petal
style
Tissues
C
a
b
c
d
e
f
D
MitoSOX fluorescence (A.U.)
0.00
10.00
20.00
30.00
40.00
50.00
60.00
*
petal
receptacle
Tissues

Figure 3

Superoxide flashes visualized by MitoSOX and flashes frequency

A. Isolated mitochondria labeled with MitoSOX red. B. Time-lapse images (upper) and typical trace (lower panel) of superoxide flashes visualized by MitoSOX red. C. Different types of traces of superoxide flashes (a) low variation slope traces, (b) high variation slope traces, (c) multi- event traces. D. Comparison of superoxide flashes frequency in petal and style of *M. denudata* (a). Comparison of superoxide flashes frequency in petal and receptacle of *N. nucifera* (b). Scale bar: 5μm.

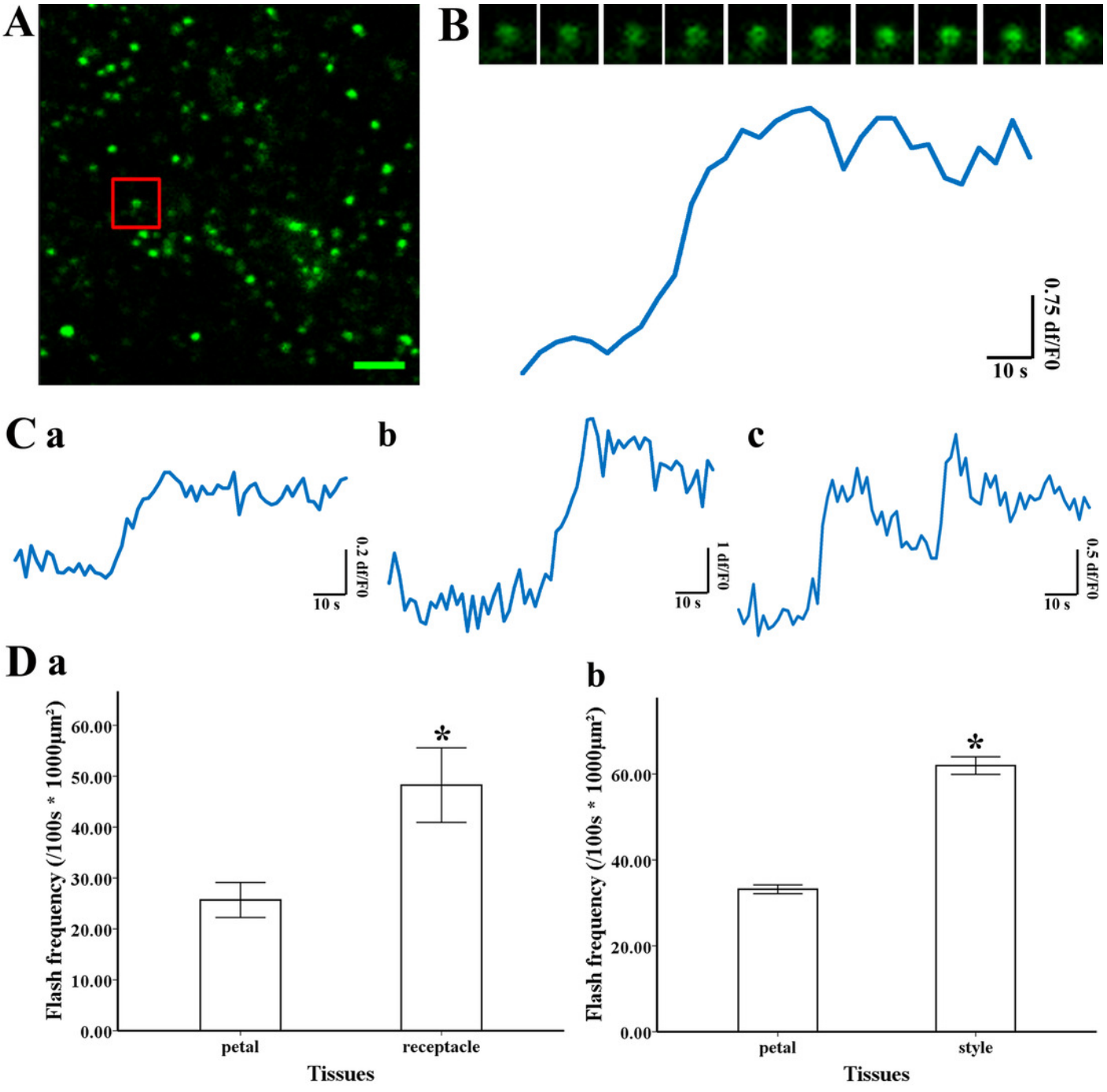
A
B
0.75 df/F0
10 s
C a
0.2 df/F0
10 s
b
1 df/F0
10 s
c
0.5 df/F0
10 s
D a
Flash frequency (/100s * 1000μm²)
60.00
50.00
40.00
30.00
20.00
10.00
0.00
*
petal
receptacle
Tissues
b
Flash frequency (/100s * 1000μm²)
60.00
40.00
20.00
0.00
*
petal
style
Tissues

Figure 4

Depolarization of mitochondria membrane potential (ΔΨm) and frequency

A. Isolated mitochondria labeled by TMRM. B. Time-lapse images (upper) and typical trace (lower panel) of depolarization of ΔΨm labeled by TMRM. C. Different types of trace of TMRM (a) instantaneous loss and recovery of ΔΨm, (b) instantaneous loss with the short period of stability before recovery of ΔΨm (c) multi-event traces. D. Comparison of depolarization of ΔΨm frequency in petal and style of *M. denudata*. (a). Comparison of depolarization of ΔΨm frequency in petal and receptacle of *N. nucifera* (b). Scale bar: 5μm.

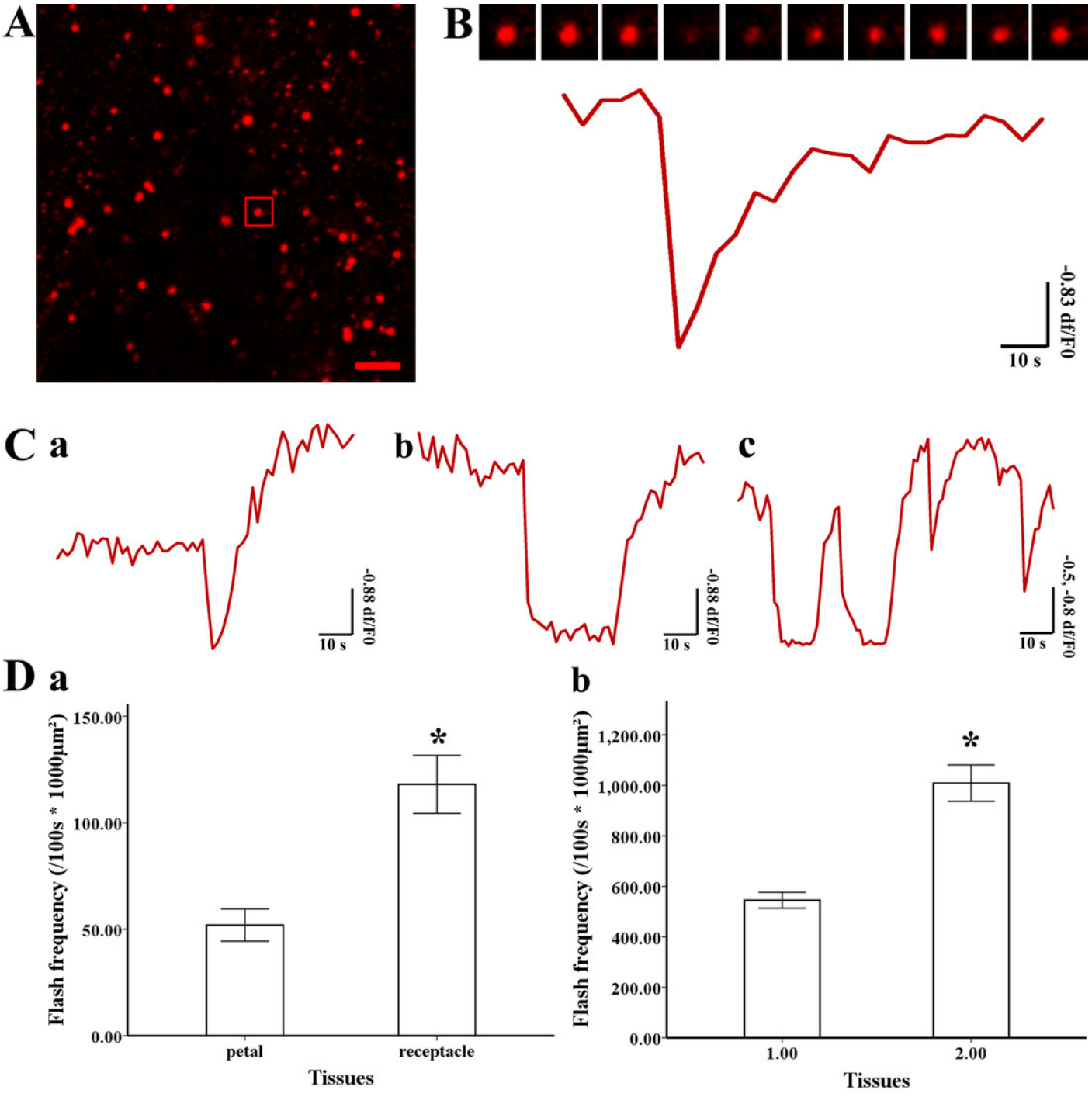
A
B
-0.83 df/F0
10 s
C a
-0.88 df/F0
10 s
b
-0.88 df/F0
10 s
c
-0.5, -0.8 df/F0
10 s
D a
Flash frequency (/100s * 1000μm²)
150.00
100.00
50.00
0.00
*
petal
receptacle
Tissues
b
Flash frequency (/100s * 1000μm²)
1,200.00
1,000.00
800.00
600.00
400.00
200.00
0.00
*
1.00
2.00
Tissues

Table 1(on next page)

Respiratory function of isolated mitochondria with our method A and previous method B

Values are mean ± S.D., n=6.

1

2

Table 1

Respiratory function of isolated mitochondria with our method A and previous method B

Groups	State 3 nmol O·min^{-1}·mg^{-1}	State 4 nmol O·min^{-1}·mg^{-1}	RCR
Stigma (*M. denudata*)	269.68±28.49	60.08±6.13	4.49±0.20^{a}
Petal (*M. denudata*)	276.06±31.50	64.46±7.88	4.29±0.16^{ab}
Receptacle (*N.nucifera*)	257.73±34.91	60.00±8.59	4.30±0.21^{ab}
Petal (*N.nucifera*)	259.14±33.82	61.99±8.68	4.19±0.25^{b}
Method B	243.90±35.01	61.89±8.39	3.94±0.18^{c}

Values are mean ± S.D., n=6.

3

4